

江西武功山早古生代花岗岩的岩石学、 锆石 U-Pb 和 Lu—Hf 同位素地球 化学特征及其地质意义



张垚垚^{1, 2)}, 刘凯¹⁾, 何庆成¹⁾, 童珏³⁾, 邓岳飞⁴⁾, 余成华⁵⁾, 孙军亮²⁾,
余廷溪^{1, 2)}, 郭骏瀚¹⁾, 王书训²⁾

1) 中国地质科学院, 北京, 100037; 2) 中国地质大学(北京), 北京, 100083;
3) 江西省地质局第四地质大队, 江西萍乡, 337000;
4) 建设综合勘察研究设计院有限公司, 北京, 100007;
5) 深圳市勘察研究院有限公司, 广东深圳, 518000

内容提要: 武功山造山带位于华夏地块与扬子地块碰撞缝合带南侧, 记录了新元古代以来的多次构造运动。本文对其中的黑云母二长花岗岩和二云母二长花岗岩进行了全面的矿物学、岩石地球化学、锆石 U-Pb 同位素年代学及 Lu—Hf 同位素研究。LA-ICP-MS 锆石 U-Pb 同位素年代学研究指示武功山黑云母二长花岗岩和二云母二长花岗岩结晶于早志留世(441.6~442.2 Ma)。武功山早志留世花岗岩具有富硅(SiO_2 含量为 67.43%~73.06%)、富碱($\text{Na}_2\text{O}+\text{K}_2\text{O}$ 含量为 6.47%~8.46%)、贫钙($\text{CaO}=0.78\% \sim 2.64\%$)、贫镁($\text{MgO}=0.46\% \sim 1.61\%$)等特征, 为强过铝质高钾钙碱性花岗岩($\text{A/CNK}=1.09 \sim 1.35$)。同时, 岩相学和地球化学指示岩石属于亚碱性系列, 分异程度较低, ΣREE 较低, 轻重稀土分异程度较高, 为 S 型花岗岩且岩浆源区物相为角闪石+斜长石+石榴子石。结合花岗岩锆石 $f_{\text{Lu/Hf}}$ 值均小于 -0.9, $\varepsilon_{\text{Hf}}(t)$ 均为负值(-6.7 到 -4.8), 指示岩浆来源于古元古代古老陆壳物质, 形成于陆内造山构造背景下, 为武功山地区对武夷—云开造山运动的响应。

关键词: 武功山; 早古生代; 地球化学; Lu—Hf 同位素; 地质意义

武功山地区位于华夏地块北缘, 北接北东向的江山—绍兴断裂带(JSF), 记录了华南板块于新元古代(~880 Ma)江南造山运动完成拼合以来的大量构造事件(Charvet et al., 1996; Faure et al., 1996; Li Zhengxiang, 1998; Li Wuxian et al., 2008; Li Xianhua et al., 2009)(图1)。拼合之后, 华南板块(SCB)在显生宙主要经历了三次构造事件, 即新元古代的俯冲—碰撞—拼合, 到早古生代晚期的陆内造山, 再到中生代的陆内造山及造山后伸展(Ren Jishun and Chen Tingyu, 1989; Ren Jishun, 1991; Li Zhengxiang, 1998; Li Zhengxiang and Li Xianhua, 2007; Faure et al., 2009; Charvet et al., 2010; Li Zhengxiang et al., 2010; Charvet, 2013; Wang Dan et al., 2013)。早古生代构造运动在中国文献中传统上称为“加里东造

山运动”, 近年来又称为“武夷—云开造山运动”(Li Zhengxiang et al., 2010)或“广西造山运动”(Wang Yuejun et al., 2010, 2011)。武夷—云开造山运动以往学者研究认为其属于陆内造山类型(Wang Yuejun et al., 2007, 2011; Faure et al., 2009; Charvet et al., 2010; Li Zhengxiang et al., 2010)。前人对武功山早古生代花岗岩地质特征、岩石学、地球化学、构造变形等方面进行了研究(Faure et al., 1996; 孙岩等 1994, 1997; 舒良树等, 1998, 2000; 张芳荣, 2000; 楼法生等, 2002, 2005; 张菲菲等, 2010; Wang Yuejun et al., 2011; Zhang Feifei et al., 2012; Yu Yang et al., 2016; Zhong, et al., 2014, 2016)。然而, 依然存在年龄差异相对较大, 岩石成因、岩浆源区研究相对较少等问题。因此, 本文以武功山地区早古

注: 本文为中国地质调查项目(编号: DD20221677-2、DD20201165)、中央财政基本科研业务费项目(编号: JKY202004、JKY202011)、江西省重点研发计划项目(编号: 2020BBG72W011)和江西省地质局科技研究项目(编号: 2021AA07)的成果。

收稿日期: 2022-06-10; 改回日期: 2022-12-21; 网络首发: 2023-01-20; 责任编辑: 章雨旭。Doi: 10.16509/j.georeview.2023.01.025

作者简介: 张垚垚, 男, 1987 年生, 高级工程师, 主要从事矿田构造、区域地质调查研究工作; Email: zhangyy@cags.ac.cn。通讯作者: 刘凯, 男, 1983 年生, 正高级工程师, 主要从事区域地质调查研究工作; Email: acancer@163.com。

生代花岗岩为研究对象,进行系统的岩石学、地球化学、U-Pb同位素年代学、Lu—Hf同位素综合研究,探讨岩石成因,同时明确其源区及其形成的大地构造环境。

1 地质背景

武功山地区位于华夏地块北侧,绍兴—江山—东乡—萍乡断裂南侧。出露地层从老到新依次为南华系、震旦系、寒武系、泥盆系、石炭系、二叠系、三叠系及少量侏罗系和第四系,以震旦系—寒武系、泥盆系、石炭系—三叠系地层为主(Faure et al., 1996; 舒良树等, 1998)。震旦系自下而上划分为坝里组、老虎塘组,岩性为变质砂岩、板岩、变质粉砂岩、硅质岩,浅海—大陆斜坡相沉积。寒武系出露地层为八

村群,八村群包括牛角河组、高滩组和水石组以及温汤岩组,岩性为变质砂岩、板岩、变质粉砂岩、角岩、片岩,浅海—大陆斜坡沉积环境。泥盆系出露地层为峡山群,峡山群包括锡矿山组、余田桥组、棋子桥组、跳马洞组,岩性为白云岩、粉砂岩、泥页岩、灰岩,海陆交互相沉积。石炭系出露地层包括杨家源组、梓山组、黄龙组,岩性为粉砂岩、泥岩、灰岩、白云岩、砂岩、砾岩,滨海沉积环境。二叠系地层包括栖霞组、小江边组、茅口组、南港组、乐平组、七宝山组、长兴组,岩性为灰岩、粉砂岩、泥岩、硅质岩,浅海相沉积。三叠系出露地层为铁石口组、安源组,岩性为砾岩、砂砾岩、砂岩、粉砂岩、炭质泥岩夹煤层或煤线,海陆交互相沉积。第四系主要为黏土、粉黏土夹碎石,河流—残坡积相沉积^①。

区内构造发育,主要分为褶皱和断裂(图2)。褶皱变形主要有三期,第一期形成于加里东早期;第二期形成于加里东晚期,叠加了印支期变形;第三期属燕山—喜马拉雅期的产物(Li Zhengxiang, 1998; Faure et al., 2009; Charvet, 2013)。武功山地区断裂构造比较发育,不同时代、不同层次、不同类型的断裂散布于区内岩石、地层中,按其变形性质及特点分为韧性剪切带和脆性断裂两类。区内发育有多个大型韧性剪切带,如温塘—邹家里—白云韧性剪切带、青茅山韧性剪切带。相对于韧性剪切带来说,区内脆性断裂更为发育,包括岩下一白马滑覆断裂、金鸡山—板上滑覆断裂、田鸡—焦坑推覆断裂、温汤断裂、岭布—易家田断裂和浒坑—洪江断裂等。

花岗岩类岩石分布广泛,早古生代(加里东期)、晚中生代(燕山期)均有发育,主要岩石类型包括似斑状花岗岩、片麻状花岗岩、花岗质眼球状片麻岩、花岗闪长岩和黑云母花岗岩等,以及少量二云母花岗岩和白云母花岗岩等(Faure et al., 2009)。武功山岩体侵入于震旦系、寒武系变质地层中,并被三江、青龙山—浒坑、明月山等燕山期岩体所侵入。武功山花岗岩体核部为似斑状花岗岩,边缘为片麻状花岗岩和花岗质眼球状片麻岩带,出露宽度2~5 km。野外调查发现,边缘带中近南北走向的糜棱面理和拉伸线理非常发育,韧性剪切作用和各种运动学标志十分明显;石英斑晶和基质均强烈变形,形成拉长压扁颗粒、波状消光、核幔构造、动力重结晶亚颗粒等各种韧性显微构造。岩体内接触带含有大量的围岩捕虏体、暗色包体等,它们均呈大小不等的扁豆状、透镜状、条带状平行展布,定向排列十分明显,其长短轴之比一般在4~6之间,有的达10以上,显

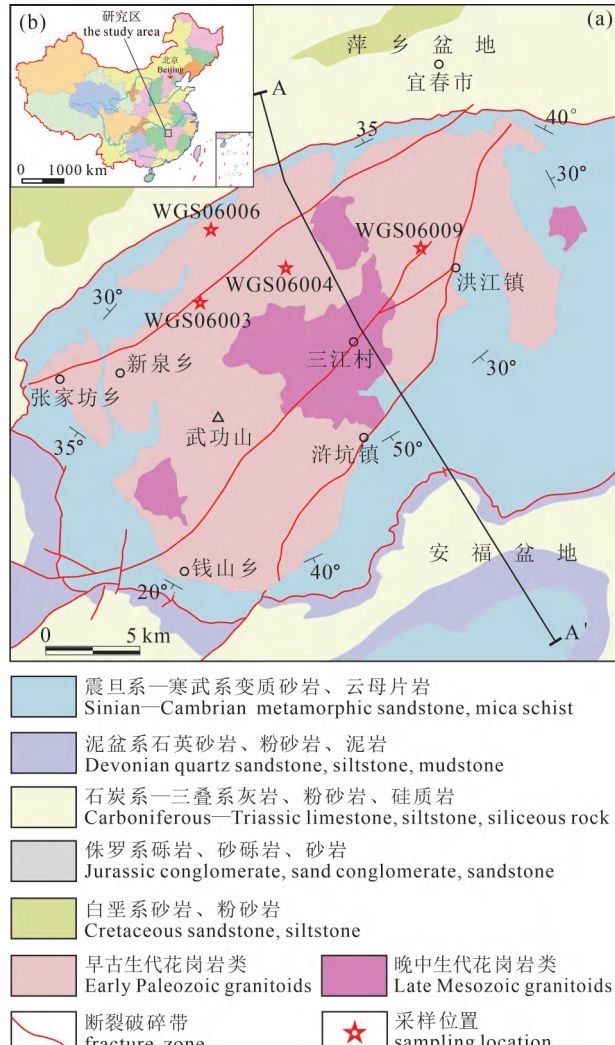


图1 武功山区域地质简图(a)及研究区位置(b)

Fig. 1 Simplified regional geological map of Wugong Mountain area (a) and the location of the study area in China (b)

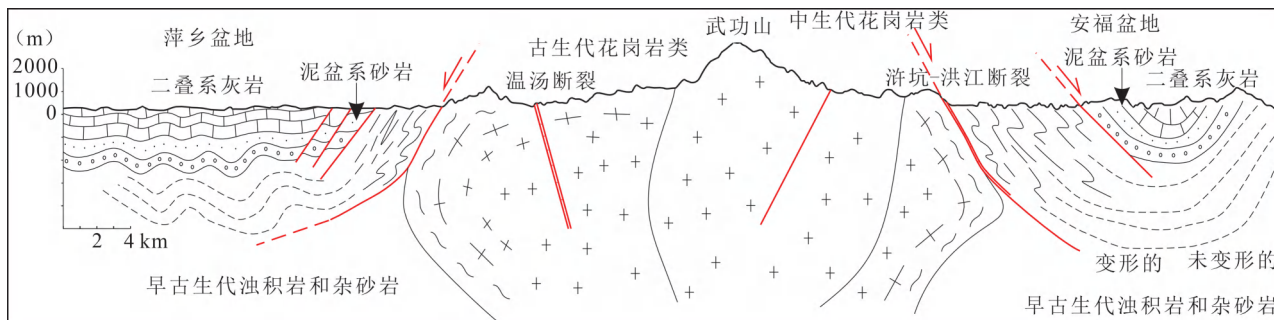


图 2 横穿萍乡盆地—武功山—安福盆地剖面图(位置见图 1 A—A')(据舒良树等,1998 修改)

Fig. 2 Cross section through Pingxiang Basin—Wugong Mountain—Anfu Basin(located on A—A' in Fig. 1)
(modified from Shu Liangshu et al., 1998&)

示出强烈变形的特点,岩石中眼球状构造、片麻状构造发育,岩石普遍具糜棱岩化,面理、线理十分普遍。

2 样品特征和实验方法

在系统地质调查的基础上,本次工作对武功山不同位置的样品进行采集分析,代表性岩性描述如下:

糜棱岩化黑云母二长花岗岩(WGS06003):岩石呈绿灰色,具变余花岗结构,变余糜棱结构,片麻状构造(图3c)。岩石由斜长石、钾长石、变余长石糜棱物、石英、黑云母、白云母组成。斜长石呈半自形板状—他形粒状,其粒径一般在0.4~3.0 mm范围内变化,与钾长石混杂集合体多呈条带状等聚集定向分布,具较强绢云母化、黝帘石化、绿帘石化,含量约20%。钾长石主要呈近半自形板状,少量他形粒状,粒径多为2~5 mm,与斜长石混杂在一起定向分布,为微斜长石,具高岭石化;常见粒内有斜长石、黑云母等嵌布,交代斜长石,可见波状消光、似鱼状、断裂等变形现象,含量15%~20%。变余长石糜棱物呈他形粒状,粒径在0.05~0.3 mm之间变化,为长石糜棱物经变质重结晶的产物,以斜长石为主;集合体主呈弯曲条纹状、线纹状等聚集定向分布,颗粒间呈三结点紧密镶嵌状,含量30%~35%。石英主要呈他形粒状,粒径一般为0.05~1.0 mm之间,粒内显波状、带状消光,含量20%~25%。黑云母、白云母呈鳞片—叶片状,直径一般<1.0 mm,二者混杂集合体呈条纹状、弯曲条纹状、线纹状等聚集定向分布,黑云母具绿泥石化,黑云母含量5%~10%,白云母含量约1%。

糜棱岩化二云母二长花岗岩(WGS06004):岩石呈灰白色,具鳞片粒状变晶结构,变余花岗结构,

片麻状构造(图3b)。岩石主由斜长石、钾长石、石英、黑云母、白云母组成,其中长石、石英、云母各自相对聚集呈条纹状相间定向排列。斜长石呈近半自形板状—他形粒状,粒径一般在0.05~2.0 mm范围内变化,与钾长石混杂集合体主呈条纹状、条带状等聚集定向分布,具绢云母化、高岭土化等;被钾长石蚕蚀状交代可见蠕虫结构,含量30%~35%。钾长石呈近半自形板状—他形粒状,粒径在0.05~2.0 mm之间,主要与斜长石混杂定向分布,为微斜长石,具高岭石化;有的粒内有斜长、文象状石英嵌布,交代斜长石,含量30%~35%。较少量细粒变晶集合体可拼合出近半自形板状钾长石外形。石英呈他形粒状,粒径在0.1~3.0 mm,集合体主要呈似透镜状、条纹状等聚集,显拉长定向特征,粒内具波状、带状消光,含量约25%。黑云母、白云母呈鳞片—叶片状,直径多<1.0 mm,二者混杂集合体主要呈条纹状、线纹状聚集定向分布;黑云母显棕色,多色性明显,具绿泥石化等,含量约10%。白云母交代黑云母。

糜棱岩化细粒斑状二云母二长花岗岩(WGS06006):岩石呈灰白色,鳞片粒状变晶结构,变余花岗结构,片麻状构造。岩石主要由斜长石、钾长石、变余长石糜棱物、石英、黑云母、白云母组成。斜长石呈近半自形板状—他形粒状,粒径一般在0.2~1.8 mm之间,与钾长石混杂集合体多呈条带状等聚集定向分布,具绢云母化、高岭石化,部分可隐约见环带,可见被钾长石蚕蚀状等交代见蠕虫结构;部分颗粒显似鱼状、机械双晶、弯曲状、断裂状、波状消光等变形现象,含量15%~20%。钾长石主要呈近半自形板状,少量他形粒状,粒径2~9 mm,与斜长石混杂在一起定向分布,为微斜长石,具高岭石化,常见粒内有斜长石、黑云母等嵌布,交代斜长



图3 武功山地区早古生代花岗岩野外及镜下照片: (a) 熔棱岩化斑状二云母二长花岗岩野外照片; (b) 熔棱岩化二云母二长花岗岩手标本; (c) 熔棱岩化黑云母二长花岗岩镜下特征; (d) 熔棱岩化斑状二云母二长花岗岩镜下特征

Fig. 3 Field and microscopic photographs of the Early Paleozoic granite in Wugong Mountain area: (a) Field photograph of mylonitized porphyritic two-mica monzogranite; (b) hand specimen of mylonitized two-mica monzogranite; (c) microscopic characteristic of mylonitized biotite monzogranite; (d) microscopic characteristic of mylonitized porphyritic two-mica monzogranite

Qtz—石英条带; Kf—钾长石残斑; FMM—变余长石云母熔棱物; Bi—黑云母; Mu—白云母

Qtz—quartz; Kf—K-feldspar remnant phenocryst; FMM—palimpsest feldspar mica mylonite; Bi—biotite; mu—Muscovite

石; 可见波状消光、似鱼状、断裂等变形现象, 有的颗粒边缘见应力蠕虫结构, 含量 30%~35%。变余长石熔棱物呈微粒状, 粒径一般<0.2 mm, 为长石熔棱物经变质重结晶的产物, 包括斜长石、钾长石; 集合体主呈弯曲条纹状、线纹状等聚集定向分布, 颗粒间呈三结点紧密镶嵌状, 含量约 20%。石英主要呈他形粒状, 少量似竹节状, 粒径在 0.1~0.7 mm 之间, 含量 20%~25%。黑云母、白云母呈鳞片—叶片状, 直径<0.2 mm, 二者混杂集合体呈条纹状、弯曲条纹状、线纹状等聚集定向分布; 黑云母显深棕色, 多色性明显, 具绿泥石化等; 大颗粒云母为变余残斑, 显似鱼状、弯曲状、膝折等变形现象, 小颗粒云母为变

余熔棱物, 含量 5%~10%。

糜棱岩化斑状二云母二长花岗岩 (WGS06009): 岩石呈灰白色, 具变余似斑状结构, 变余糜棱结构, 片麻状构造、糜棱纹理构造(图 3a、d)。岩石由斜长石、钾长石、石英、黑云母、白云母组成。斜长石多呈他形粒状, 少量为近半自形板状, 粒径在 0.3~1.0 mm 范围内变化, 与钾长石混杂集合体多呈条带状等聚集定向分布, 颗粒间呈三结点紧密镶嵌状, 具绢云母化、高岭石化, 含量 35%~40%。钾长石主要呈近半自形板状, 少量他形粒状, 粒径多为 2~18 mm, 与斜长石混杂在一起定向分布, 为微斜长石, 具高岭石化; 常见粒内有斜长石、黑

云母等嵌布,交代斜长石,含量 30%~35%。石英多呈他形粒状,粒径一般 0.1~3.0 mm,集合体主呈弯曲条带状、条纹状聚集定向分布,粒内显波状、带状消光,含量 20%~25%。黑云母、白云母呈鳞片—叶片状,直径一般<1.0 mm,二者混杂集合体呈条纹状、弯曲条纹状、线纹状等聚集定向分布;黑云母显深棕色,多色性明显,局部绿泥石化,含量 5%~10%,黑云母略多。

样品主量元素、稀土元素、微量元素分析在河北省区域地质调查院实验室完成。主量元素测试仪器为 Axiosmax X 射线荧光光谱仪;灼失量、 H_2O^- 、 H_2O^+ 分析仪器为 P245 电子分析天平;FeO 采用 50 mL 滴定管滴定;稀土元素及微量元素分析测试仪器为 X Serise 2 等离子体质谱仪。测试温度为 26°C, 湿度为 40%, 相对误差小于 5%。

锆石分选和制靶在河北省区域地质调查院实验室完成,透反射及阴极荧光(CL)在北京锆年领航科技有限公司完成,锆石年龄分析测试在北京锆年领航科技有限公司完成。分析仪器为 Finnigan Neptune 型 MC-ICP MS 及配套的 New Wave UP213 激光剥蚀系统。激光剥蚀束斑直径为 25 μm,剥蚀深度为 20~40 μm,频率为 10 Hz,能量密度为 2.5 J/cm²,以 He 为载气。信号较小的²⁰⁷Pb、²⁰⁶Pb、²⁰⁴Pb

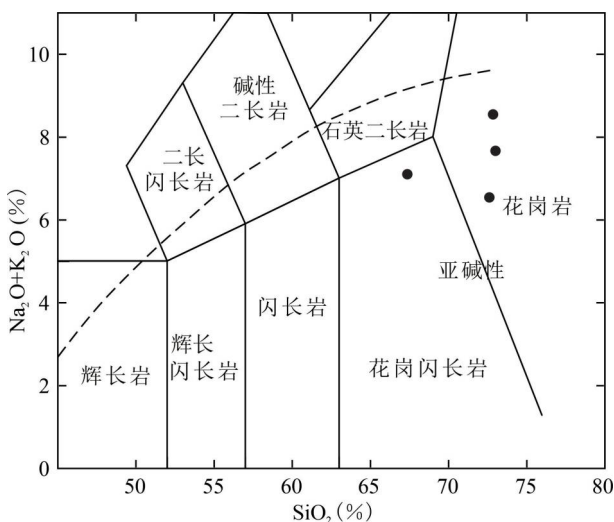


图 4 武功山早古生代花岗岩 TAS 分类图解
(底图据 Middlemost, 1994)

Fig. 4 TAS diagram of the Early Paleozoic granite in Wugong Mountain area (after Middlemost, 1994)

Ir—Irvine 分界线,上方为碱性,下方为亚碱性

(Irvine and Baragar, 1971)

The Ir—Irvine boundary is alkaline at the top and subalkaline at the bottom (Irvine and Baragar, 1971)

(⁺²⁰⁴Hg)、²⁰²Hg 用离子计数器(multi-ion-counters)接收,²⁰⁸Pb、²³²Th、²³⁸U 信号用法拉第杯接收,实现了所有目标同位素信号的同时接受。详细的仪器操作见(侯可军等,2009)。

锆石 Hf 同位素测试在北京锆年领航科技有限公司完成。分析仪器为 Finnigan Neptune 型多接收等离子质谱仪上进行的,激光剥蚀系统为美国 Newwave UP213, ICP-MS 为 Agilent7500a。激光器波长为 213 nm,激光束斑直径为 35 μm,采用 He 为剥蚀物质载气。校正用外标样为 Plesovice(年龄为 337±0.37 Ma)(Sláma et al., 2008),普通铅校正采用 ComPbCorr #3.17 校正程序(Andersen, 2002)。Hf 的地幔模式年龄计算中,亏损地幔 $n(^{176}\text{Hf})/n(^{177}\text{Hf})$ 现在值采用 0.28325, $n(^{176}\text{Lu})/n(^{177}\text{Hf})$ 采用 0.0384(Griffin et al., 2000),地壳模式年龄计算时采用平均地壳的 $n(^{176}\text{Lu})/n(^{177}\text{Hf}) = 0.015$ (Griffin et al., 2002)。

3 测试结果

3.1 主量元素

武功山花岗岩四个样品烧失量(0.53%~1.59%)较低,总量为 99.82%~99.92%,受后期流体及变质作用影响较小,岩石地球化学特征能够有效反应岩石特征(表 1)。样品 SiO_2 含量为 67.43%~73.06%,为酸性岩; TiO_2 含量 0.21%~0.46%; Al_2O_3 含量 14.03%~15.43%; Fe_2O_3 含量为 0.45%~1.22%; FeO 含量为 0.85%~1.97%; MgO 含量为 0.46%~1.61%; K_2O 含量为 3.37%~5.50%; Na_2O 含量 2.86%~3.65%; $\text{Na}_2\text{O}+\text{K}_2\text{O}$ 含量为 6.47%~8.46%。TAS 图解中,样品投点于花岗岩、花岗闪长岩区域,属于亚碱性系列(图 4)。 K_2O — SiO_2 图解(图 5)中样品投点于高钾钙碱性系列区域。岩石分异指数 DI 为 77.12~90.75,分异程度较低,铝饱和指数 A/CNK 为 1.09~1.35,A/NK 为 1.38~1.69,为强过铝质岩石(图 6)。

3.2 稀土元素

武功山花岗岩稀土含量较低,变化范围相对较小, ΣREE 为 95.48×10^{-6} ~ 179.00×10^{-6} ,轻稀土 LREE 含量为 85.85×10^{-6} ~ 162.52×10^{-6} ,重稀土 HREE 含量为 9.63×10^{-6} ~ 17.16×10^{-6} (表 1)。轻/重稀土比值为 7.49~9.86,(La/Yb)_N 为 7.91~12.69,轻重稀土分异程度较高;轻稀土分异程度较高;重稀土分异程度较低; δEu 为 0.50~0.86,具中等—弱负异常; δCe 为 1.04~1.10,具弱正异常。

表1 武功山花岗岩主量元素(%)、稀土元素($\times 10^{-6}$)、微量元素($\times 10^{-6}$)组成Table 1 Major elements(%) ,trace elements($\times 10^{-6}$) and REE elements($\times 10^{-6}$) compositions of granite in Wugong Mountain area

样品编号	06003	06004	06006	06009	样品编号	06003	06004	06006	06009	样品编号	06003	06004	06006	06009	
SiO ₂	67.43	72.69	72.92	73.06	A/NK	1.6	1.69	1.38	1.44	Nd	23.4	22.0	25.3	30.3	
Al ₂ O ₃	15.43	14.03	14.43	14.38	A/CNK	1.09	1.24	1.35	1.2	Sm	4.93	4.09	5.20	6.19	
Fe ₂ O ₃	1.22	0.45	0.62	0.48	AR	2.27	2.08	2.28	2.38	Eu	1.26	0.82	0.48	0.93	
FeO	1.97	1.59	0.85	1.21	R1	2352	2927	2484	2650	Gd	4.11	3.30	3.91	5.26	
MnO	0.075	0.051	0.032	0.035	R2	678	577	391	487	Tb	0.66	0.47	0.57	0.84	
TiO ₂	0.46	0.29	0.21	0.22	V	62.8	34.2	14.6	18.4	Dy	3.55	2.25	2.78	4.51	
CaO	2.64	2.32	0.78	1.67	Co	8.69	5.04	2.02	2.70	Ho	0.66	0.37	0.46	0.80	
MgO	1.61	1.02	0.46	0.50	Ba	727	411	282	552	Er	1.85	1.11	1.27	2.20	
Na ₂ O	3.65	2.86	2.97	3.28	Hf	4.13	3.64	3.87	4.48	Tm	0.29	0.18	0.18	0.34	
K ₂ O	3.37	3.61	5.50	4.31	Ga	17.5	16.8	18.4	16.8	Yb	1.97	1.24	1.19	2.20	
P ₂ O ₅	0.150	0.101	0.155	0.070	Nb	11.7	10.0	15.9	11.4	Lu	0.32	0.21	0.18	0.33	
烧失	1.59	0.71	0.89	0.53	Rb	135	170	311	175	Y	20.2	11.6	13.6	23.7	
总和	99.82	99.90	99.92	99.89	Sr	294	151	60.8	104	Σ REE	139.47	121.27	142.28	178.99	
Q	25.24	37.48	34.77	34.09	Ta	1.21	1.22	1.59	0.90	LREE	126.06	112.15	131.73	162.52	
An	12.35	8.19	0.67	5.41	Th	14.3	15.4	24.2	19.7	HREE	13.42	9.12	10.55	16.47	
Ab	31.54	22.63	23.34	27.52	U	2.78	8.81	4.20	2.34	LREE	9.40	12.30	12.49	9.87	
Or	20.34	21.41	32.64	25.57	Zr	150	132	122	144	HREE	(La/Yb) _N	10.43	15.42	16.18	12.72
C	1.36	2.76	3.74	2.42	Ni	9.31	6.37	1.81	3.38	δ Eu	0.86	0.68	0.32	0.50	
Hy	6.12	4.71	1.91	2.77	La	28.6	26.6	26.9	38.9	δ Ce	1.10	1.03	1.22	1.05	
DI	77.12	81.53	90.75	87.18	Ge	61.3	52.6	67.0	77.7						
SI	13.57	10.68	4.42	5.13	Pr	6.50	5.91	6.80	8.51						

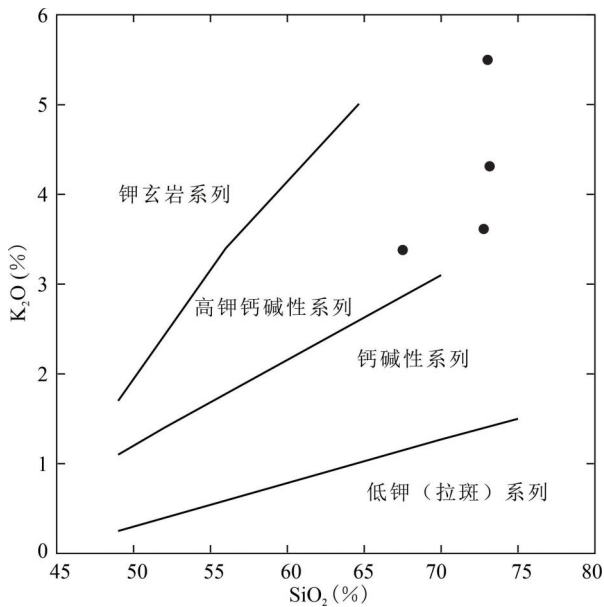
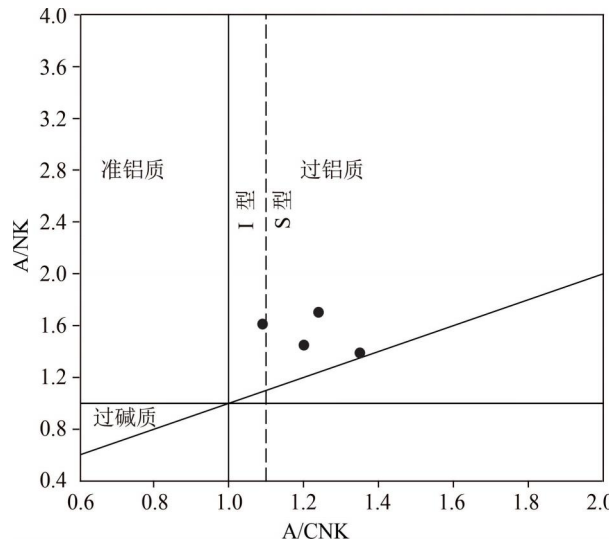
图5 武功山早古生代花岗岩 K_2O — SiO_2 图解
(底图据 Middlemost, 1985)Fig. 5 K_2O — SiO_2 diagram of the Early Paleozoic granite in Wugong Mountain area (after Middlemost, 1985)图6 武功山早古生代花岗岩 A/NK—A/CNK 图解
(据 Maniar and Piccoli, 1989)

Fig. 6 A/NK—A/CNK diagram of the Early Paleozoic granite in Wugong Mountain area (after Maniar and Piccoli, 1989)

$$A/NK = \frac{n(Al_2O_3)}{n(Na_2O) + n(K_2O)}; A/CNK = \frac{n(Al_2O_3)}{n(CaO) + n(Na_2O) + n(K_2O)}$$

3.3 微量元素

武功山花岗岩微量元素含量变化较大。微量元素蛛网图(图8)显示,武功山花岗岩不同样品具有

相似的分布形态,总体表现为右倾型式,表现为多峰谷“W”型模式。显示富集大离子亲石元素 Rb 及高

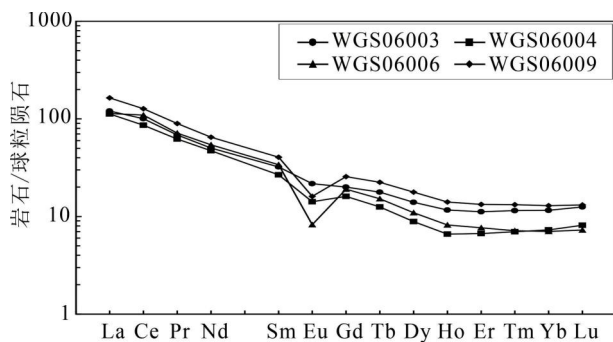


图 7 武功山早古生代花岗岩稀土元素球粒陨石标准化配分型式(标准化数据据 Sun and McDonough, 1989)

Fig. 7 Chondrite-normalized REE patterns of the Early Paleozoic granite in Wugong Mountain area (normalization values from Sun and McDonough, 1989)

场强元素 Th、U 及稀土元素 La、Ce。与相邻元素相比, 样品明显亏损 Ba、Sr、Nb、Ti、P, 与壳源型花岗岩相似。Sr、Ba、Ti 的明显亏损, 暗示岩浆结晶过程中斜长石与含 Ti 的矿物(如黑云母)发生了明显的分离结晶作用。

个样品稀土配分曲线分布基本相同, 具右倾特征, 轻稀土相对富集、重稀土相对亏损(图 7)。重稀土元素较为平缓, 具有弱的分馏或分馏不明显。较低的 $(\text{La/Yb})_{\text{N}}$ 比值、平缓的重稀土分布模式及低的 Sr/Y 比值暗示岩浆来源较浅。

3.4 锆石 U-Pb 年龄

黑云母二长花岗岩 WGS06003 测试的锆石自形

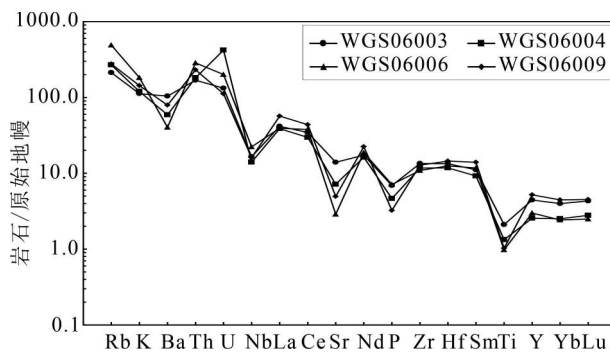


图 8 武功山早古生代花岗岩微量元素原始地幔标准化蛛网图(标准化数据据 Sun and McDonough, 1989)

Fig. 8 Primitive mantle-normalized trace element spider diagrams of the Early Paleozoic granite in Wugong Mountain area (normalization values after Sun and McDonough, 1989)

程度良好, 多数为长柱状, 阴极发光图像显示锆石发育振荡环带, 具岩浆成因特征(Rubatto and Gebauer, 2000)。选择不发育裂隙和包裹体的锆石进行年龄测试(图 9)。剔除个别捕获锆石后, 锆石 Pb 含量 $19.1 \times 10^{-6} \sim 72.8 \times 10^{-6}$, Th 含量 $112.5 \times 10^{-6} \sim 428.1 \times 10^{-6}$, U 含量 $225.8 \times 10^{-6} \sim 943.0 \times 10^{-6}$ (表 2)。Th/U 比值 $0.21 \sim 0.71$, 比值 > 0.1 , 为岩浆成因锆石(Cleasson et al., 2000; Belousova et al., 2002)。本样品 U-Pb 年龄 < 1.0 Ga, 因而采用锆石 $^{206}\text{Pb}/^{238}\text{U}$ 年龄(Griffin et al., 2004)。样品锆石 $^{206}\text{Pb}/^{238}\text{U}$ 呈点群分布, 分布较为集中, 年龄值为 $437.9 \pm 5.8 \sim 444.2 \pm 6.0$ Ma, 谐和年龄为 441.6 ± 1.2 Ma, MSWD = 4.6, 加

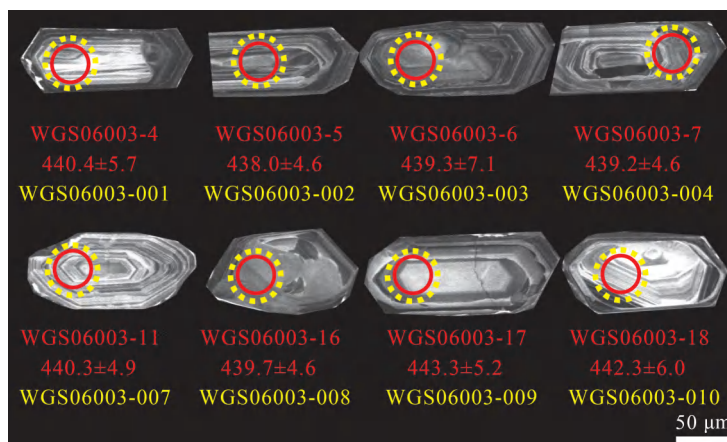


图 9 武功山黑云母二长花岗岩(WGS06003)锆石阴极发光照片及 U-Pb 年龄谐和图

Fig. 9 Cathodoluminescence (CL) images and LA-ICP-MS U-Pb concordia diagram of the zircons from biotite monzogranite (WGS06003) in Wugong Mountains area

图中实心圆为锆石 U-Pb 测年位置; 虚线圆圈为 Hf 同位素分析位置。图中标准年龄为 $n(^{206}\text{Pb}) / n(^{238}\text{U})$ 年龄

Filled circles in the figure represent the zircon U-Pb dating position; dotted circles are the locations of

Hf isotope analysis. The age is $n(^{206}\text{Pb}) / n(^{238}\text{U})$ ages

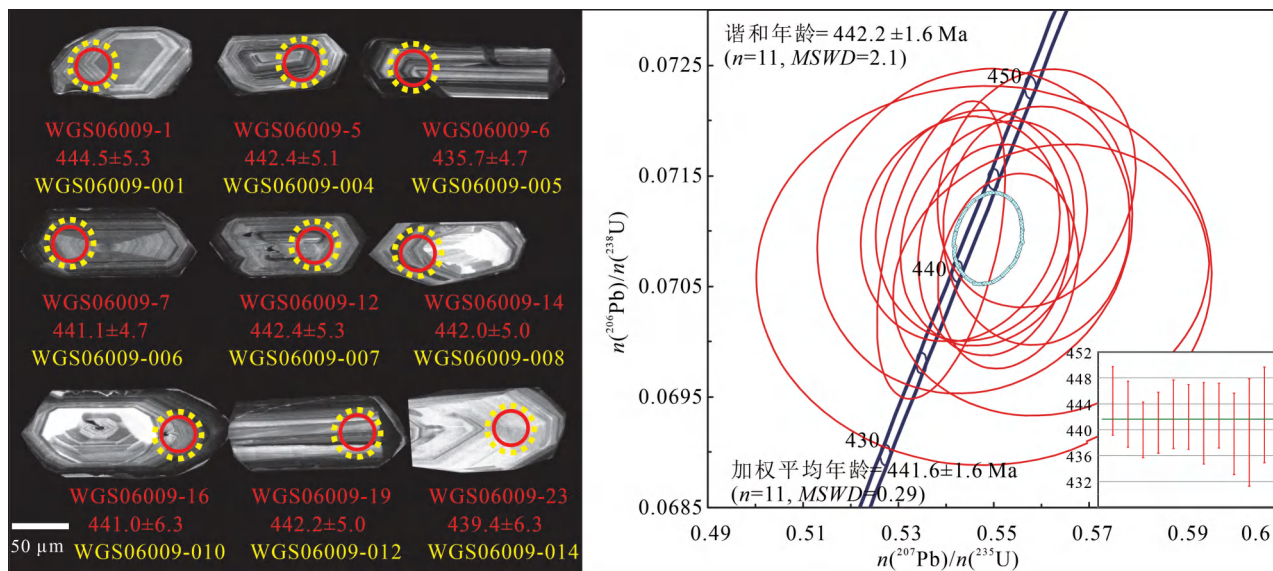


图10 武功山二云母二长花岗岩(WGS06009)锆石阴极发光照片及U-Pb年龄协和图

Fig. 10 Cathodoluminescence (CL) images of zircons and LA-ICP-MS zircon U-Pb concordia diagram of two-mica monzogranite (WGS06009) in Wugong Mountains area

图中实心圆圈为锆石U-Pb测年位置;虚线圆圈为Hf同位素分析位置。图中标准年龄为 $n(^{206}\text{Pb})/n(^{238}\text{U})$ 年龄

Filled circles in the figure represent the zircon U-Pb dating position;dotted circles are the locations of

Hf isotope analysis. The age is $n(^{206}\text{Pb})/n(^{238}\text{U})$ ages

权平均值为 440.8 ± 1.2 Ma, MSWD=0.70(图9)。

二云母二长花岗岩WGS06009测试的锆石自形程度较好,均为长柱状,振荡环带发育,具岩浆成因特征(Rubatto and Gebauer, 2000)。选择不发育裂隙和包裹体的锆石进行年龄测试,在发育振荡环带的位置打点(图10)。个别测试锆石为捕获锆石或打点精度不足,导致所测年龄远离一致曲线,选择剔除。锆石Pb含量 $4.1\times10^{-6}\sim89.1\times10^{-6}$, Th含量 $21.1\times10^{-6}\sim278.5\times10^{-6}$, U含量 $50.3\times10^{-6}\sim1144.0\times10^{-6}$ (表2)。Th/U值 $0.19\sim0.56$,比值 >0.1 ,显示岩浆成因锆石(Cleasson et al., 2000; Belousova et al., 2002)。本样品U-Pb年龄 <1.0 Ga,因而采用锆石 $^{206}\text{Pb}/^{238}\text{U}$ 年龄(Griffin et al., 2004)。样品锆石 $^{206}\text{Pb}/^{238}\text{U}$ 呈点群分布,分布较为集中,年龄值为 $439.4\pm6.3\sim444.5\pm5.3$ Ma,谐和年龄为 442.2 ± 1.6 Ma, MSWD=2.1,加权平均值为 441.6 ± 1.6 Ma, MSWD=0.29(图10)。

3.5 锆石Lu—Hf同位素组成

黑云母二长花岗岩WGS06003锆石 $n(^{176}\text{Lu})/n(^{177}\text{Hf})$ 值为 $0.000718\sim0.002357$, $n(^{176}\text{Lu})/n(^{177}\text{Hf})$ 值较小,表明锆石在形成后,仅具有少量的放射性成因Hf积累,因而可以用初始 $n(^{176}\text{Hf})/n(^{177}\text{Hf})$ 值代表形成时的Hf同位素组成(吴福元等,2007a)。

等,2007a)。 $n(^{176}\text{Hf})/n(^{177}\text{Hf})$ 初始比值和 $\varepsilon_{\text{Hf}}(t)$ 值根据同一锆石U-Pb测年数据计算;二阶段模式年龄($t_{\text{DM}2}$)根据亏损幔源计算(Griffin et al., 2000)。测定结果显示,测试点锆石Hf同位素 $n(^{176}\text{Hf})/n(^{177}\text{Hf})$ 值较为稳定,比值为 $0.282321\sim0.282376$ (表3), $n(^{176}\text{Yb})/n(^{177}\text{Hf})$ 值为 $0.018854\sim0.063988$, $f_{\text{Lu/Hf}}$ 为 $-0.98\sim-0.93$,锆石 $\varepsilon_{\text{Hf}}(t)$ 为 $-6.7\sim-4.8$,变化范围较小,表明岩体来源较为单一(图11)。锆石Hf单阶段模式年龄($t_{\text{DM}1}$)为 $1257\sim1343$ Ma,二阶段模式年龄($t_{\text{DM}2}$)为 $1726\sim1844$ Ma。

二云母二长花岗岩WGS06009锆石 $n(^{176}\text{Lu})/n(^{177}\text{Hf})$ 值为 $0.000808\sim0.002585$, $n(^{176}\text{Lu})/n(^{177}\text{Hf})$ 值较小,表明锆石在形成后,仅具有少量的放射性成因Hf积累,因而可以用初始 $n(^{176}\text{Hf})/n(^{177}\text{Hf})$ 值代表形成时的Hf同位素组成(吴福元等,2007a)。 $n(^{176}\text{Hf})/n(^{177}\text{Hf})$ 初始比值和 $\varepsilon_{\text{Hf}}(t)$ 值根据同一锆石U-Pb测年数据计算;二阶段模式年龄($t_{\text{DM}2}$)根据亏损幔源计算(Griffin et al., 2000)。测定结果显示,测试点锆石Hf同位素 $n(^{176}\text{Hf})/n(^{177}\text{Hf})$ 值较为稳定,比值为 $0.282196\sim0.282305$ (表3), $n(^{176}\text{Yb})/n(^{177}\text{Hf})$ 值为 $0.024741\sim0.071393$, $f_{\text{Lu/Hf}}$ 为 $-0.98\sim-0.92$,锆石 $\varepsilon_{\text{Hf}}(t)$ 为 $-11.0\sim-7.5$,变化范围较小,表明岩体来源较为

表 2 武功山花岗岩 LA-ICP-MS 锆石同位素分析结果

Table 2 Zircon LA-ICP-MS analytical results of granite in Wugongshan area

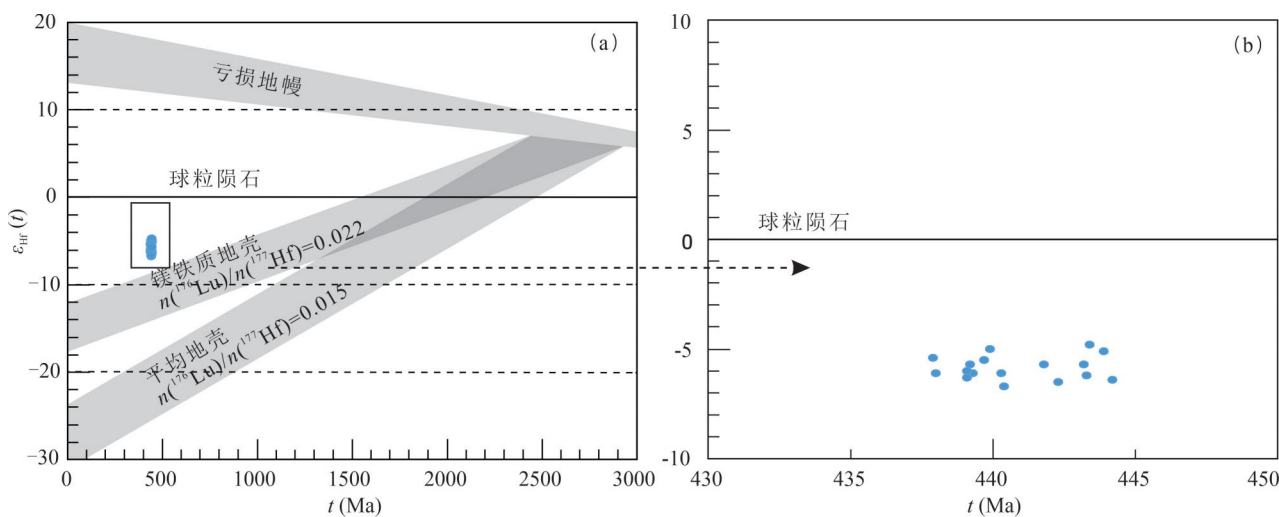
测点号	元素含量($\times 10^{-6}$)			同位素比值						同位素年龄(Ma)							
	Pb	Th	U	Th/U	$n(^{207}\text{Pb})/n(^{206}\text{Pb})$		$n(^{207}\text{Pb})/n(^{235}\text{U})$		$n(^{207}\text{Pb})/n(^{238}\text{U})$		$n(^{206}\text{Pb})/n(^{235}\text{U})$	$n(^{206}\text{Pb})/n(^{238}\text{U})$	测值	2σ			
					测值	2σ	测值	2σ	测值	2σ							
WGS06003-4	19.13	160.6	225.8	0.71	0.05782	0.0024	0.5653	0.0238	0.07071	0.0009	468.2	89.3	452.4	15.1	441.4	5.7	95
WGS06003-5	41.22	112.5	543.0	0.21	0.05615	0.0013	0.5452	0.0118	0.07031	0.0008	428.7	50.3	441.8	7.4	438.1	4.6	99
WGS06003-6	72.82	428.1	943.0	0.45	0.05471	0.0010	0.5349	0.0133	0.07053	0.0012	394.5	45.2	434.9	9.0	439.3	7.1	98
WGS06003-7	56.73	222.9	713.0	0.31	0.05565	0.0009	0.5401	0.0101	0.07052	0.0008	427.4	37.6	438.8	6.8	439.2	4.6	99
WGS06003-9	25.74	116.2	303.9	0.38	0.05673	0.0020	0.5623	0.0190	0.07135	0.0010	440.3	77.1	451.3	12.1	444.2	6.0	99
WGS06003-10	66.89	358.0	822.0	0.44	0.05615	0.0010	0.5456	0.0099	0.07049	0.0007	439.3	41.5	442.3	6.5	439.1	4.1	99
WGS06003-11	27.52	180.8	328.8	0.55	0.05657	0.0017	0.5510	0.0152	0.07068	0.0008	433.3	65.1	444.6	10.0	440.3	4.9	98
WGS06003-16	31.55	176.0	378.7	0.46	0.05672	0.0016	0.5522	0.0150	0.07064	0.0008	442.8	61.1	445.2	9.9	439.7	4.6	98
WGS06003-17	23.26	161.8	279.4	0.58	0.05704	0.0017	0.5593	0.0163	0.07118	0.0009	451.7	65.3	449.4	10.1	443.3	5.2	99
WGS06003-18	56.94	294.6	727.0	0.41	0.05526	0.0013	0.5421	0.0142	0.07103	0.0010	397.5	51.2	439.1	9.2	442.3	6.3	99
WGS06003-21	59.35	354.5	718.0	0.49	0.05588	0.0011	0.5441	0.0111	0.07064	0.0007	424.3	47.4	440.8	7.3	439.9	4.6	99
WGS06003-22	50.41	241.1	624.7	0.39	0.05635	0.0013	0.5544	0.0128	0.07118	0.0008	450.5	51.1	447.7	8.3	443.2	4.8	98
WGS06003-26	48.44	386.8	558.0	0.69	0.05681	0.0013	0.5593	0.0123	0.07130	0.0008	459.4	51.2	450.5	8.1	443.9	4.7	99
WGS06003-27	29.13	179.9	347.4	0.52	0.05672	0.0014	0.5559	0.0141	0.07121	0.0008	451.2	54.9	449.2	9.2	443.4	4.9	98
WGS06003-28	55.54	316.2	678.0	0.47	0.05613	0.0010	0.5468	0.0113	0.07047	0.0009	442.2	43.6	441.8	7.4	439.1	5.2	99
WGS06003-29	32.63	220.3	391.0	0.56	0.05627	0.0019	0.5437	0.0180	0.07029	0.0010	429.3	76.2	440.5	12.0	437.9	5.8	99
WGS06003-30	30.54	227.5	358.0	0.64	0.05579	0.0015	0.5463	0.0123	0.07094	0.0008	410.0	59.1	441.9	9.5	441.8	4.7	99
WGS06009-1	20.32	92.18	258.6	0.36	0.05683	0.0017	0.5589	0.0169	0.07139	0.0009	442.9	65.7	448.8	11.3	445.2	5.3	99
WGS06009-5	26.72	145.7	319.3	0.46	0.05564	0.0017	0.5457	0.0167	0.07105	0.0008	395.3	67.6	440.8	11.3	442.9	5.1	97
WGS06009-6	34.41	184.3	426.1	0.43	0.05668	0.0013	0.5528	0.0118	0.07064	0.0007	454.5	50.7	446.2	8.3	440.4	4.4	99
WGS06009-7	32.57	132.4	416.9	0.32	0.05577	0.0013	0.5503	0.0134	0.07083	0.0008	431.6	53.1	445.3	8.4	441.6	4.7	99
WGS06009-12	28.84	137.2	357.2	0.38	0.05732	0.0017	0.5589	0.0159	0.07105	0.0009	465.5	65.7	449.5	10.2	443.0	5.4	99
WGS06009-14	31.53	155.8	384.1	0.41	0.05611	0.0016	0.5498	0.0158	0.07098	0.0008	430.3	62.0	445.8	10.1	442.8	5.1	99
WGS06009-16	89.12	217.7	1144	0.19	0.05554	0.0011	0.5391	0.0111	0.07083	0.0011	423.3	41.0	437.7	7.4	441.7	6.4	98
WGS06009-19	43.23	278.5	494.3	0.56	0.05557	0.0018	0.5433	0.0172	0.07102	0.0008	395.9	69.8	439.2	11.2	442.8	5.0	99
WGS06009-23	9.924	61.21	118.8	0.51	0.05793	0.0028	0.5387	0.0167	0.07056	0.0010	440.6	100.1	448.3	18.2	440.2	6.3	97
WGS06009-25	4.107	21.12	50.32	0.42	0.05646	0.0041	0.5617	0.0267	0.07061	0.0014	330.9	150.3	431.7	26.2	440.3	8.3	99
WGS06009-26	7.632	47.23	91.60	0.52	0.05643	0.0029	0.5482	0.0390	0.07099	0.0012	370.8	110.8	439.5	18.2	442.7	7.4	97

表3 武功山花岗岩锆石LA-ICP-MS Lu—Hf分析结果

Table 3 LA-ICP-MS Lu—Hf analysis results of granite in Wugong Mountain area

样品编号	年龄 (Ma)	$\frac{n(^{176}\text{Yb})}{n(^{177}\text{Hf})}$	$\frac{n(^{176}\text{Lu})}{n(^{177}\text{Hf})}$	$\frac{n(^{176}\text{Hf})}{n(^{177}\text{Hf})}$	$\varepsilon_{\text{Hf}}(0)$	$\varepsilon_{\text{Hf}}(t)$	t_{DM1} (Ma)	t_{DM2} (Ma)	$f_{\text{Lu/Hf}}$
WGS06003-001	440.4	0.039295	0.001401	0.282321	-15.9	-6.7	1328	1844	-0.96
WGS06003-002	438.0	0.041951	0.001448	0.282338	-15.3	-6.1	1306	1809	-0.96
WGS06003-003	439.3	0.044410	0.001573	0.282339	-15.3	-6.1	1309	1808	-0.95
WGS06003-004	439.2	0.018854	0.000718	0.282344	-15.1	-5.7	1273	1781	-0.98
WGS06003-005	444.2	0.034170	0.001249	0.282326	-15.8	-6.4	1316	1828	-0.96
WGS06003-006	439.1	0.049199	0.001800	0.282336	-15.4	-6.3	1321	1819	-0.95
WGS06003-007	440.3	0.027308	0.001022	0.282333	-15.5	-6.1	1298	1811	-0.97
WGS06003-008	439.7	0.044515	0.001682	0.282358	-14.6	-5.5	1286	1767	-0.95
WGS06003-009	443.3	0.040135	0.001394	0.282332	-15.6	-6.2	1312	1818	-0.96
WGS06003-010	442.3	0.061009	0.002175	0.282330	-15.6	-6.5	1343	1837	-0.93
WGS06003-011	439.9	0.063988	0.002357	0.282376	-14.0	-5.0	1283	1739	-0.93
WGS06003-012	443.2	0.046039	0.001684	0.282350	-14.9	-5.7	1297	1783	-0.95
WGS06003-013	443.9	0.040008	0.001448	0.282364	-14.4	-5.1	1269	1747	-0.96
WGS06003-014	443.4	0.041775	0.001507	0.282374	-14.1	-4.8	1257	1726	-0.95
WGS06003-015	439.1	0.029244	0.001094	0.282337	-15.4	-6.0	1295	1804	-0.97
WGS06003-016	437.9	0.040165	0.001464	0.282358	-14.6	-5.4	1278	1764	-0.96
WGS06003-017	441.8	0.054415	0.001912	0.282351	-14.9	-5.7	1304	1786	-0.94
WGS06009-001	444.5	0.042310	0.001663	0.282258	-18.2	-8.9	1427	1987	-0.95
WGS06009-004	442.4	0.049732	0.001890	0.282247	-18.6	-9.4	1452	2017	-0.94
WGS06009-005	440.0	0.044603	0.001652	0.282249	-18.5	-9.3	1439	2010	-0.95
WGS06009-006	441.1	0.024741	0.000808	0.282254	-18.3	-8.9	1401	1983	-0.98
WGS06009-007	442.4	0.040858	0.001459	0.282251	-18.4	-9.1	1429	2000	-0.96
WGS06009-008	442.0	0.044508	0.001641	0.282218	-19.6	-10.4	1483	2077	-0.95
WGS06009-010	441.0	0.071393	0.002585	0.282265	-17.9	-9.0	1453	1990	-0.92
WGS06009-012	442.2	0.042452	0.001490	0.282242	-18.7	-9.5	1443	2021	-0.96
WGS06009-014	439.4	0.040667	0.001522	0.282261	-18.1	-8.9	1418	1981	-0.95
WGS06009-016	439.6	0.026939	0.000986	0.282196	-20.4	-11.0	1488	2116	-0.97
WGS06009-017	442.3	0.063466	0.002361	0.282305	-16.5	-7.5	1386	1896	-0.93

注:表中各参数的计算公式和常数同周晓萍等(2022)。

图11 武功山黑云母二长花岗岩(WGS06003)锆石 $\varepsilon_{\text{Hf}}(t)$ — t 图(底图据吴福元等,2007a)Fig. 11 $\varepsilon_{\text{Hf}}(t)$ versus age diagram of biotite monzogranite (WGS06003) in Wugong Mountains area

(Base image from Wu Fuyuan et al., 2007a&b)

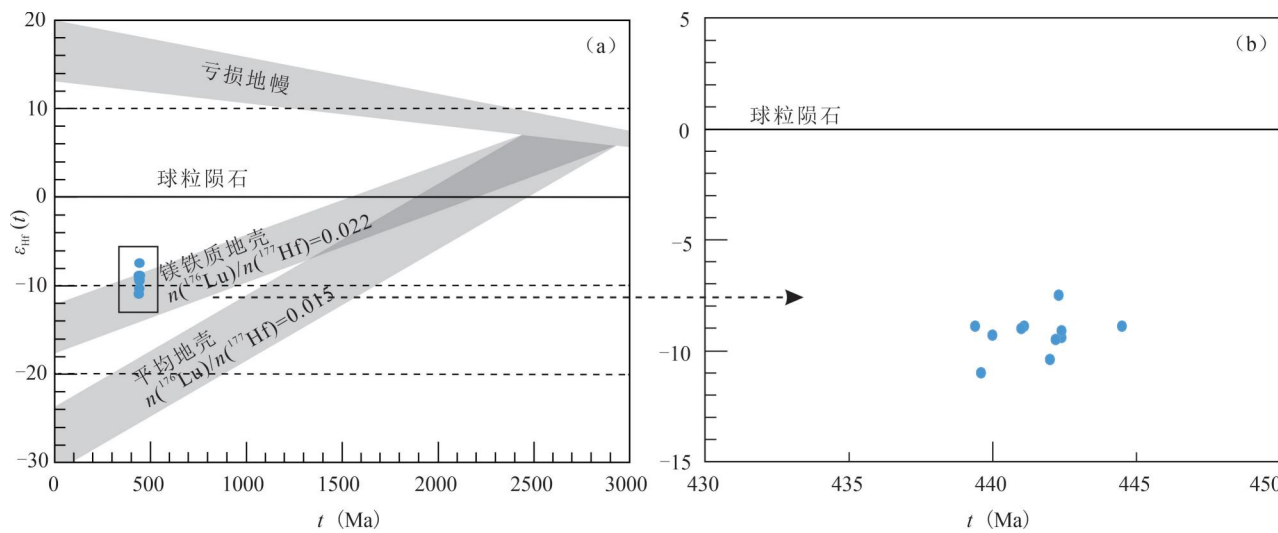


图 12 武功山二云母二长花岗岩(WGS06009)锆石 $\varepsilon_{\text{Hf}}(t)$ — t 图(底图据吴福元等, 2007a)

Fig. 12 $\varepsilon_{\text{Hf}}(t)$ versus age diagram of two-mica monzogranite (WGS06009) in Wugong

Mounttains area (Base image from Wu Fuyuan et al. , 2007a&)

单一(图 12)。锆石 Hf 单阶段模式年龄(t_{DM1})为 1386~1488 Ma, 二阶段模式年龄(t_{DM2})为 1896~2116 Ma。

4 讨论

4.1 年龄意义

已有学者对武功山地区早古生代花岗岩进行过年代学研究。获得的武功山片麻状花岗岩锆石 U-Pb 年龄为 $428.0 \pm 1.1 \sim 462.3 \pm 2.3$ Ma (楼法生等, 2005), 455 ± 8 Ma、 424 ± 6 Ma、 455 ± 9 Ma (Wang Yuejun et al. , 2011); 张家坊岩体年龄为 427.9 ± 1.2 Ma (楼法生等, 2005), 440 ± 2 Ma (Zhang Feifei et al. , 2012), 438 ± 3 Ma (Yu Yang et al. , 2016), 444 ± 3 Ma, 448 ± 3 Ma (Zhong Yufang et al. , 2016); 山庄岩体年龄为 460.5 ± 1.5 Ma (楼法生等, 2005), 424 ± 3 Ma (张菲菲等, 2010)。这些结果表明武功山早古生代花岗岩年龄为 $424 \pm 6 \sim 462.3 \pm 2.3$ Ma, 时代跨度较大。本次测试选择武功山具有代表性花岗岩进行年龄测试, 测试方法为 LA-ICP-MS, 测试结果为谐和年龄 $441.6 \pm 1.2 \sim 442.2 \pm 1.6$ Ma, 加权平均值为 $440.8 \pm 1.2 \sim 441.6 \pm 1.6$ Ma, 表明武功山花岗岩形成于早志留世。结合前人研究成果, 表明武功山地区早古生代花岗岩年龄大致集中于三个时期, 分别为 455 Ma、440 Ma 和 425 Ma, 且大致具由东向西年龄逐渐降低的趋势。

沿江山—绍兴断裂带, 区域上也存在着大量相

同时代的花岗岩。半山铺花岗闪长岩锆石 U-Pb 年龄为 418 ± 2 Ma (张菲菲等, 2010); 432 ± 3 Ma (Guan Yili et al. , 2014)。红霞桥岩体锆石 U-Pb 年龄为 423 ± 6 Ma (张菲菲等, 2010), 434 ± 3 Ma (Guan Yili et al. , 2014)。凤顶山花岗岩锆石 U-Pb 年龄为 436 ± 5 Ma (Zhong Yufang et al. , 2013)。乐安花岗岩体锆石 U-Pb 年龄为 429 ± 2 Ma, 双庄岩体锆石 U-Pb 年龄为 441 ± 6 Ma, 彭公庙岩体锆石 U-Pb 年龄为 405 ± 3 Ma, 万阳山岩体锆石 U-Pb 年龄为 433 ± 4 Ma, 塘湖岩体锆石 U-Pb 年龄为 454 ± 2 Ma (Zhang Feifei et al. , 2012)。本次测试数据结合已有研究成果表明, 武夷—云开造山运动范围较大, 持续时间较长, 武功山地区早志留世花岗岩为该运动影响下本区的响应。

4.2 岩石成因和源区特征探讨

武功山花岗岩镜下组成矿物中未见富铁云母、碱性角闪石等特征碱性暗色矿物, $10000\text{Ga}/\text{Al}$ 分别为 2.14~2.41, 均小于 2.6, 稀土配分曲线呈右倾, Zr 含量为 $121.73 \times 10^{-6} \sim 150.50 \times 10^{-6}$, $\text{Zr}+\text{Nb}+\text{Ce}+\text{Y}$ 为 $205.75 \times 10^{-6} \sim 256.28 \times 10^{-6}$, 与 A 型花岗岩特征 (Collins et al. , 1982; Whalen et al. , 1987; Sylvester, 1998) 差异较大。黑云母二长花岗岩和二云母二长花岗岩中含有大量原生白云母和黑云母, 均不含角闪石, 标准矿物计算 (CIPW) 中不含有透辉石, 标准矿物刚玉分子 (C) 为 1.36~3.74, 表明花岗岩具 S 型特征, 与 I 型花岗岩特征 (吴福元等,

2007b)不符。在 A/NK—A/CNK 判别图中,所有点均投入 I—S 型花岗岩分界的 S 型一侧(图 6)。综上认为武功山花岗岩为 S 型花岗岩。

在部分熔融的过程中,如无外来物质加入 Nb/Ta 比值变化较小,同源岩浆 Nb/Ta 比值相同(Foley, 1984; Barth et al., 2000)。武功山花岗岩 Nb/Ta 比值分别为 8.14~12.68,远小于地幔平均值(60),接近于地壳平均值(10)(Wedepohl, 1995),且变化幅度小,表明岩浆源区为壳源物质,岩浆源区成分较为均一。 δEu 为 0.50~0.86,表明岩浆形成过程中发生了较为明显的斜长石分离结晶作用,同时也表明武功山花岗岩岩浆主要来源于上地壳物质。过渡金属元素 V、Co、Ni 含量分别为 14.6~62.8、2.02~8.69、1.81~9.31。V 接近于上部地壳含量,Co、Ni 均低于上部地壳含量(V、Co、Ni 上部地壳含量分别为 55、11.6、18.6, Wedepohl, 1995);但 V 远低于下部地壳含量(V 下部地壳含量为 149, Wedepohl, 1995)。以上特征表明武功山花岗岩岩浆主要是上地壳物质部分熔融形成的,岩浆形成过程

没有明显的幔源物质加入。

不同源区的的锆石通常具有不同的 Hf 同位素特征,因而可以借助 Hf 同位素探讨岩浆源区特征(Vervoort et al., 1996; Amelin et al., 2000; Griffin et al., 2002; Kinny and Mass, 2003)。武功山花岗岩 $f_{\text{Lu/Hf}}$ 为 -0.98~-0.92 明显小于大陆地壳(-0.72, Vervoort et al., 1996)。二阶段模式年龄可以真实反映其源区物质从亏损地幔被抽取的时间(即其源区物质在地壳的平均存留年龄)(Nebel et al., 2007)。武功山花岗岩锆石 Hf 单阶段模式年龄(t_{DM})分别为 1257~1343 Ma, 1386~1488 Ma, 二阶段模式年龄(t_{DM2})分别为 1726~1844 Ma, 1896~2116 Ma。锆石 $\varepsilon_{\text{Hf}}(t)$ 全部为负值(-6.7~-4.8),除个别点投影于 1.8 Ga 趋势演化线附近外,其他点均投影于 1.8 Ga 和 2.5 Ga 趋势演化线之间,表明岩浆源区为演化的古元古代陆壳物质。

研究认为,花岗岩中的 Sr 和 Y 元素含量及比值与其岩浆源区残留相关系密切(Defant and Drummond, 1990)。稀土元素中 Yb、Lu 在石榴子石

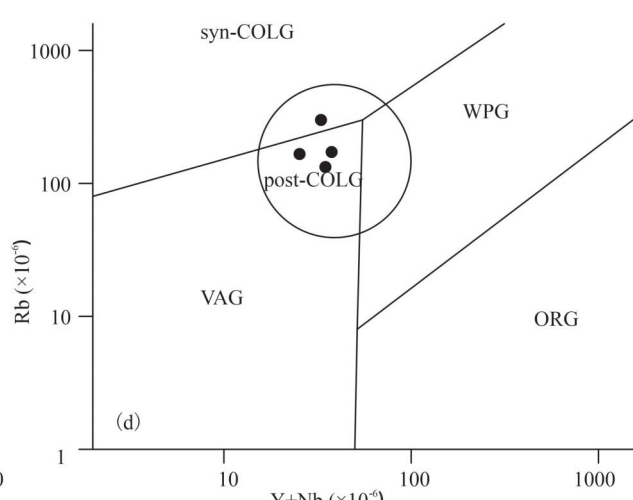
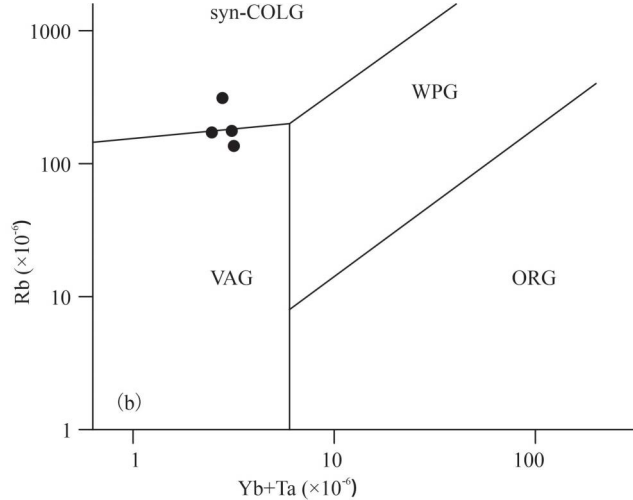
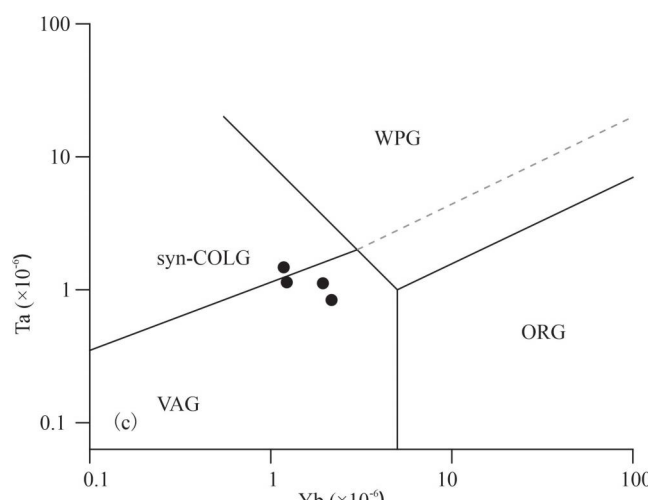
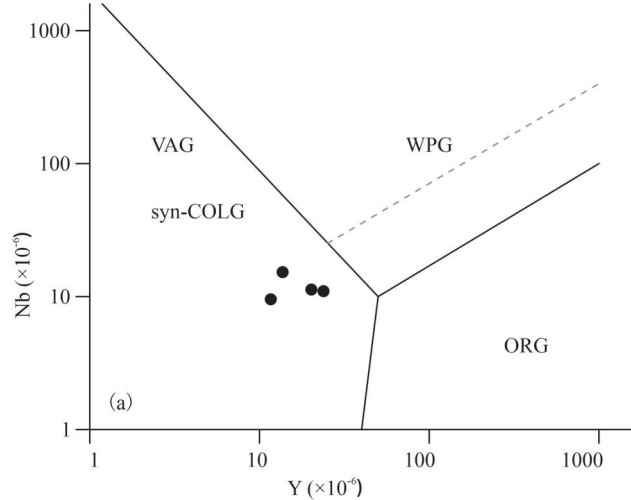


图 13 武功山花岗岩类微量元素构造环境判别图解(底图据 Pearce et al. , 1984) : (a) Nb—Y 图解;
(b) Rb—(Yb+Ta) 图解;(c) Ta—Yb 图解;(d) Rb—(Y+Nb) 图解

Fig. 13 Tectonic discrimination diagrams for the granite in Wugong Mountains area (Base map from Pearce et al. , 1984) : (a) Nb vs. Y diagram; (b) Rb vs. (Yb+Ta) diagram; (c) Ta vs. Yb diagram ;(d) Rb vs. (Y+Nb) diagram
Syn-COLG—同碰撞花岗岩; Post-COLG—后碰撞花岗岩; VAG—火山岛弧花岗岩; WPG—板内花岗岩; ORG—洋脊花岗岩
Syn-COLG—syn-collision granite; Post-COLG—post-collision granite; VAG—volcanic arc granite; WPG—within plate granite;
ORG—ocean ridge granite

中的分配系数最大,Dy 和 Ho 在角闪石中的分配系数最大(Sisson, 1994)。部分熔融过程中,Nb、Ta 残留于角闪石,Ti 残留于金红石,(Rollisonhr, 1993)。当岩浆源区残留相中石榴子石含量达 10% 时,其部分熔融形成的花岗岩具高锶低钇特征(Hollocher et al. , 2002)。岩浆源区残留相以角闪石为主,Y/Yb 接近 10,若以石榴子石为主,比值明显大于 10(葛小月等,2002)。武功山花岗岩稀土配分曲线表明,重稀土配分较为平缓,Y/Yb 比值分别为 9.38~11.43 接近 10,岩体不具有 Adakite(高锶低钇中酸性岩)特征,石榴子石为岩体组成矿物,表明岩浆源区以角闪石为主,含少量石榴子石。武功山花岗岩均具有 δEu 异常(0.32~0.86),表明岩浆源区存在斜长石。综合分析认为岩浆源区残留相为角闪岩相,残留矿物组合为角闪石+斜长石+石榴子石。

4.3 构造环境及地质意义背景探讨

扬子地块和华夏地块之间的古生物地层和古生态演化是相关和连续的,寒武纪和奥陶纪地层表现

为从华夏地块的浅海硅质碎屑序列向扬子地块东部的层间碳酸盐—硅质碎屑序列过渡,以及向扬子地块中部的浅水碳酸盐为主的序列过渡(Wang Yuejun et al. , 2010)。区域未见早古生代蛇绿岩套或弧岩浆作用,因而武夷—云开造山运动为陆内造山事件(Ren Jishun, 1991; Faure et al. , 2009; Charvet et al. , 2010; Li Zhengxiang et al. , 2010; Wang Yuejun et al. , 2007, 2011)。持续时间为中奥陶世(>460 Ma)至早泥盆世(约 415 Ma)(Li Zhengxiang et al. , 2010)。Yu Yang 等(2016)研究认为张家坊岩体形成于陆内造山环境,Zhong Yufang 等(2013)认为凤顶山花岗岩形成于陆内造山环境。高场强元素(HFSE)因不易受热液蚀变和低于角闪岩相变质作用的影响,可以有效判别岩石构造环境(Pearce and Cann, 1973)。样品 Nb—Y 构造判别图解(图 13a)中,样品投点于火山弧—同碰撞造山环境;Rb—(Yb+Ta) 图解(图 13b)中,样品投点于火山弧与同碰撞边界处;Ta—Yb 图解(图 13c)中,样品投点于同碰

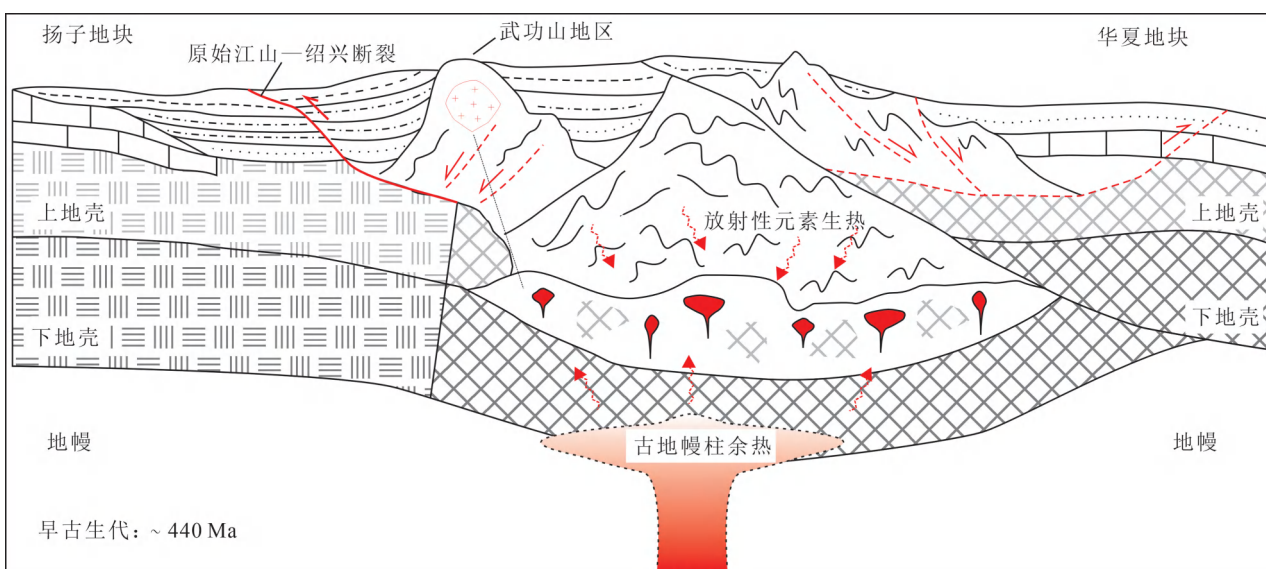


图 14 早古生代武功山地区深部构造概念模型(据 Li Zhengxiang et al. , 2010 修改)

Fig. 14 Conceptual model of deep tectonics in the Wugong Mountain area during Early Paleozoic
(modified from Li Zhengxiang et al. , 2010)

撞和火山弧区域;Rb-(Y+Nb)图解(图13d)中,样品投点于火山弧一同碰撞造山环境。因此,武功山花岗岩形成于陆内造山运动。

早古生代,受武夷—云开造山运动的影响,华夏地块与扬子地块碰撞拼贴,江山—绍兴断裂带的地壳进一步加厚,古元古代沉积物中放射性元素衰变产生的热量,加上区域上新元古代地幔柱活动的余热,使过厚地壳热成熟(Li Xianhua et al., 2008; Li Zhengxiang et al., 2010),造成了沉积物的脱水部分熔融,可能也造成了华夏地块基底岩石的部分熔融。随着造山运动的加剧,造山带发生垮塌,岩浆沿构造薄弱部位上升侵位于地壳浅部,最终形成黑云母二长花岗岩和二云母二长花岗岩(图14)。

5 结论

(1)武功山花岗岩为亚碱性序列岩石,分异程度较低, Σ REE较低,轻重稀土分异程度较高,稀土配分曲线具右倾特征, δ Eu具中等—弱负异常,为S型花岗岩,岩浆源区矿物相为角闪石+斜长石+石榴子石。

(2)武功山花岗岩锆石U-Pb定年结果为 $441.6 \pm 1.2 \sim 442.2 \pm 1.6$ Ma,表明武功山花岗岩形成于早志留世。

(3)武功山花岗岩锆石 $f_{\text{Lu/Hf}}$ 为 $-0.98 \sim -0.92$,二阶段模式年龄(t_{DM2})分别为 $1726 \sim 1844$ Ma, $1896 \sim 2116$ Ma, $\varepsilon_{\text{Hf}}(t)$ 全部为负值,结合岩石地球化学特征,表明岩浆源区为演化的古元古代陆壳物质。

(4)武功山花岗岩形成于陆内造山环境,为本区在武夷—云开造山运动的响应。

注释 / Note

① 中国地质科学院. 2021. 环武功山地区地热(干热岩)资源调查评价成果报告.

参 考 文 献 / References

(The literature whose publishing year followed by a “&” is in Chinese with English abstract; The literature whose publishing year followed by a “#” is in Chinese without English abstract)

葛小月, 李献华, 陈志刚, 李伍平. 2002. 中国东部燕山期高Sr低Y型中酸性火山岩的地球化学特征及成因:对中国东部地壳厚度的制约. 科学通报, 47(6): 474~480.

侯可军, 李延河, 田有荣. 2009. LA-MC-ICP-MS锆石微区原位U-Pb定年技术. 矿床地质, 28(4): 481~492.

楼法生, 沈渭洲, 王德滋, 舒良树, 吴富江, 张芳荣, 于津海. 2005. 江西武功山穹隆复式花岗岩的锆石U-Pb年代学研究. 地质学报, 79(5): 636~644.

楼法生, 舒良树, 于津海, 王德滋. 2002. 江西武功山穹隆花岗岩石地球化学特征与成因. 地质论评, 48(1): 80~88.

舒良树, 孙岩, 王德滋, Faure M, Charvet J, Monie P. 1998. 华南武

- 功山中生代伸展构造. 中国科学(D辑), 28(5): 431~438.
- 舒良树, 王德滋, 沈渭洲. 2000. 江西武功山中生代变质核杂岩的花岗岩类Nd-Sr同位素研究. 南京大学学报(自然科学版), 36(3): 306~311.
- 孙岩, 舒良树, Faure M, Charvet J. 1994. 赣北武功山花岗岩穹窿伸展构造——中法合作考察研究新进展. 南京大学学报(自然科学版), (4): 633~637.
- 孙岩, 舒良树, Faure M, Charvet J. 1997. 赣北地区武功山变质核杂岩的构造发育. 南京大学学报(自然科学), 33(3): 447~449.
- 吴福元, 李献华, 郑永飞, 高山. 2007a. Lu-Hf同位素体系及其岩石学应用. 岩石学报, 23(2): 185~220.
- 吴福元, 李献华, 杨进辉, 郑永飞. 2007b. 花岗岩成因研究的若干问题. 岩石学报, 23(6): 1217~1238.
- 张芳荣. 2000. 武功山片麻岩特征及侵位机制. 华东地质学院学报, 23(2): 146~149.
- 张菲菲, 王跃军, 范蔚茗, 张爱梅, 张玉芝. 2010. 湘东—赣西早古生代晚期花岗岩体的LA-ICP-MS锆石U-Pb定年研究. 地球化学, 39(5): 414~426.
- 周晓萍, 吕军阳, 胡秉谦, 康恺, 姜帆, 胡亮, 张娜. 2022. 胶北地区西涝口地区牧牛山二长花岗岩锆石U-Pb和Lu-Hf同位素研究——指示华北克拉通古元古代岩浆作用及地壳演化. 地质论评, 68(3): 891~906.
- Amelin Y, Lee D C, Halliday A N. 2000. Early-middle Archean crustal evolution deduced from Lu-Hf and U-Pb isotopic studies of single zircon grains. Geochim. Cosmochim. Acta, 64: 4205~4225.
- Andersen T. 2002. Correction of common lead in U-Pb analyses that do not report ^{204}Pb . Chemical Geology, 192(1~2): 59~79.
- Barth M G, McDonough W F, Rndnick R L. 2000. Tracking the budget of Nb and Ta in the continental crust, Chem. Geol., 165: 197~213.
- Belousova E A, Griffin W L, O'Reilly S Y, Fisher N. 2002. Igneous zircon: Trace element composition as an indicator of source rock type. Contributions to Mineralogy and Petrology, 143(5): 602~622.
- Blichert-Toft J, Chauvel C, Albarède F. 1997. Separation of Hf and Lu for high-precision isotope analysis of rock samples by magnetic sector—multiple collector ICP-MS. Contributions to Mineralogy and Petrology, 127(3): 248~260.
- Charvet J, Shu Liangshu, Shi Yangshen, Guo Lingzhi, Faure M. 1996. The building of south China: Collision of Yangtze and Cathaysia blocks, problems and tentative answers. Journal of Southeast Asian Earth Sciences, 13(3~5): 223~235.
- Charvet J, Shu Liangshu, Faure M, Choulet F, Wang B, Lu Huafu, Le Breton N. 2010. Structural development of the Lower Paleozoic belt of South China: Genesis of an intracontinental orogen. Journal of Asian Earth Sciences, 39, 309~330.
- Charvet J. 2013. The Neoproterozoic—Early Paleozoic tectonic evolution of the South China Block: An overview. Journal of Asian Earth Sciences, 74, 198~209.
- Cleasson S, Vetrin V, Bayanova T, Downes H. 2000. U-Pb zircon ages from a Devonian carbonatite dyke, Kola peninsula, Russia: A record of geological evolution from the Archaean to the Palaeozoic. Lithos, 51: 95~108.
- Collins W J, Beams S D, White A J R, Chappell B W. 1982. Nature and origin of A-type granites with particular reference to southeastern Australia. Contrib. Mineral. Petrol., 80: 189~200.
- Defant M J, Drummond M S. 1990. Derivation of some morden arc magmas by young subducted lithosphere. Nature, 347: 662~665.
- Faure M, Shu Liangshu, Wang Bo, Charvet J, Choulet F, Monie P.

2009. Intracontinental subduction: A possible mechanism for the Early Palaeozoic Orogen of SE China. *Terra Nova*, 21: 360~368.
- Faure M, Sun Yan, Shu Liangshu, Monie P, Charvet J. 1996. Extensional tectonics within a subduction-type orogen. The case study of the Wugongshan dome (Jiangxi Province, southeastern China). *Tectonophysics* 263, 77~106.
- Foley S F. 1984. Liquid immiscibility and melt segregation in alkaline lamprophyres from Labrador. *Lithos*, 17: 127~137.
- Ge Xiaoyue, Li Xianhua, Chen Zhigang, Li Wuping. 2002 #. Geochemical characteristics and genesis of Yanshanian high Sr and low Y type intermediate—acid volcanic rocks in eastern China: Constraints on crustal thickness in eastern China. *Chinese Science Bulletin*, 47(6): 474~480.
- Goolaerts A, Mattielli N, Jong J D, Weis D, Scoates J S. 2004. Hf and Lu isotopic reference values for the zircon standard 91500 by MC-ICP-MS. *Chemical Geology*, 206(1~2): 1~9.
- Griffin W L, Belousova E A, Shee S R. 2004. Crustal Evolution in the northern Yilarn Craton: U-Pb and Hf-isotope evidence from detrital zircons. *Precambrian Research*, 131(3~4): 213~282.
- Griffin W L, Pearson N J, Belousova E, Jackson S E, Achterbergh E, O'Reilly S Y, Shee S R. 2000. The Hf isotope composition of cratonic mantle: LAM-MC-ICPMS analysis of zircon megacrysts in kimberlites. *Geochim. Cosmochim. Acta*, 64: 133~147.
- Griffin W L, Wang Xiang, Jackson S E, Pearson N J, O'Reilly S Y, Xu Xisheng, Zhou Xinmin. 2002. Zircon geochemistry and magma mixing, SE China: Insitu analysis of Hf isotopes, Tonglu and Pingtan igneous complexes. *Lithos*, 61: 237~269.
- Guan Yili, Yuan Chao, Sun Min, Wilde S, Long Xiaoping, Huang Xiaolong, Wang Qiang. 2014. I-type granitoids in the eastern Yangtze Block: Implications for the Early Paleozoic intracontinental orogeny in South China. *Lithos*, 206~207: 34~51.
- Hollocher, Bull J, Robinson P. 2002. Geochemistry of the metamorphosed Ordovician Taconian Magmatic Arc, Bronson Hill anticlinorium, western New England. *Physics and Chemistry of the Earth*, 27: 5~45.
- Hou Kejun, Li Yanhe, Tian Yourong. 2009&. In situ U-Pb zircon dating using laser ablation-multi ion counting-ICP-MS. *Mineral Deposits*, 28(4): 481~492.
- Irvine T N, Baragar W R A. 1971. A guide to the chemical classification of the common volcanic rocks. *Canad Earth Sci.*, 8: 523~548.
- Kinny P D, Maas R. 2003. Lu—Hf and Sm—Nd isotope systems in zircon. In: Hanchar J M, Hoskin P W O. Eds. *Zircon. Rev. Mineral. Geochem.*, 53: 327~341.
- Li Wuxian, Li Xianhua, Li Zhengxiang, Lou Fasheng. 2008. Obduction-type granites within the NE Jiangxi Ophiolite: Implications for the final amalgamation between the Yangtze and Cathaysia Blocks. *Gondwana Research* 13, 288~301.
- Li Xianhua, Li Wuxian, Li Zhengxiang, Liu Ying. 2008. 850~790 Ma bimodal volcanic and intrusive rocks in northern Zhejiang, South China: A major episode of continental rift magmatism during the breakup of Rodinia. *Lithos*, 102(1~2): 341~357.
- Li Xianhua, Li Wuxian, Li Zhengxiang, Lo Chinghua, Wang Jian, Ye Meifang, Yang Yueheng. 2009. Amalgamation between the Yangtze and Cathaysia Blocks in South China: Constraints from SHRIMP U-Pb zircon ages, geochemistry and Nd—Hf isotopes of the Shuangxiu volcanic rocks. *Precambrian Research*, 174: 117~128.
- Li Zhengxiang and Li Xianhua. 2007. Formation of the 1300-km-wide intracontinental orogen and postorogenic magmatic province in Mesozoic South China: A flat-slab subduction model. *Geology*, 35 (2): 179~182.
- Li Zhengxiang, Li Xianhua, Wartho J A, Clark C, Li Wuxian, Zhang Chuanlin, Bao Chaomin. 2010. Magmatic and metamorphic events during the Early Paleozoic Wuyi Yunkai orogeny, southeastern South China: New age constraints and pressure—temperature conditions. *Geological Society of America Bulletin*, 122: 772~793.
- Li Zhengxiang. 1998. Tectonic history of the major East Asian lithospheric blocks since the mid-Proterozoic—A synthesis. *American Geophysical Union, Geodynamics Series*, 27: 221~243.
- Lou Fasheng, Shu Liangshu, Yu Jinhai, Wang Dezi. 2002&. Petrological and geochemical characteristics and origin of the Wugongshan dome granite, Jiangxi Province. *Geological Review*, 48 (1): 80~88.
- Lou Fasheng, Shen Weizhou, Wang Dezi, Shu Liangshu, Wu Fujiang, Zhang Fangrong, Yu Jinhai. 2005&. Zircon U-Pb isotopic chronology of the Wugongshan dome compound granite in Jiangxi Province. *Acta Geologica Sinica*, 79(5): 636~644.
- Maniar P D, Piccoli P M. 1989. Tectonic discrimination of granitoids. *GSA Bulletin*, 101(5): 635~643.
- Middlemost E A K. 1985. *Magmas and Magmatic Rocks*. London: Longman: 1~266.
- Middlemost E A K. 1994. Naming materials in the magma/igneous rock system. *Earth-Science Reviews*, 37(3~4): 215~224.
- Nebel O, Nebel-Jacobsen Y, Mezger K, Berndt J. 2007. Initial Hf isotope conmpsoitions in magmatic zircon from Early Proterozoic rocks from the Gawler Craton, Australia: A test for zircon model ages. *Chemical Geology*, 241(1~2): 23~37.
- Pearce J A, Cann J R. 1973. Tectonic setting of basic volcanic rocks determined using trace element analyses. *Earth and Planetary Science Letters*, 19: 290~300.
- Pearce J A, Harris N B W, Tindle A G. 1984. Trace element discrimination diagrams for the tectonic interpretation of granitic rocks. *Journal of Petrology*, 25: 956~983.
- Ren Jishun, Chen Tingyu. 1989. Tectonic evolution of the continental lithosphere in eastern China and adjacent areas. *J. Southeast Asian Earth Sci.*, 3: 17~27.
- Ren Jishun. 1991. On the geotectonics of southern China. *Acta Geologica Sinica*, 4(2): 111~130.
- Rollison H R. 1993. *Using Geochemical Data: Evaluation, Presentation, Interpretation*. London: Longman Group U K Ltd.: 107~135.
- Rubatto D, Gebauer D. 2000. Use of Cathodoluminescence for U-Pb Zircon Dating by IOM Microprobe: Some Examples form the Western Alps. *Cathodoluminescence in Geoscience*. Berlin: Springer-Verlag: 373~400.
- Shu Liangshu, Sun Yan, Wang Dezi, Faure M, Charvet J, Monie P. 1998 #. Mesozoic extensional structure of Wugongshan, South China. *Science in China (Series D)*, 28 (5): 431~438.
- Shu Liangshu, Wang Dezi, Shen Weizhou. 2000&. Nd—Sr isotopic compositions of granitic rocks of the Mesozoic metamorphic core complex in the Wugongshan area, Jiangxi Province. *Journal of Nanjing University (Natural Sciences)*, 36(3): 306~311.
- Sisson T W. 1994. Hornblende—melt trace-element partitioning measured by ion microprobe. *Chem. Geol.*, 117: 331~344.
- Sláma J, Koler J, Condon D J, Crowley J L, Gerdes A, Hanchar J M, Horstwood M S, Morris G A, Nasdala L, Norberg N. 2008. Plešovice zircon — A new natural reference material for U-Pb and Hf isotopic microanalysis. *Chemical Geology*, 249(1~2): 1~35.
- Soderlund U, Patchett P J, Vervoort J D, Isachsen C E. 2004. The ^{176}Lu decay constant determined by Lu—Hf and U-Pb isotope systematic of Precambrian mafic intrusions. *Earth and Planetary Science Letters*, 219: 311~324.

- Sun S S, McDonough W F. 1989. Chemical and isotopic systematics of ocean basalts: Implications for mantle composition and processes. Geological Society of London and Blackwell Scientific Publications, London: 313~345.
- Sun Yan, Shu Liangshu, Faure M, Charvet J. 1994&. Extensional structure of the granite dome of the Wugongshan Mountain in the northern Jiangxi Province. *Journal of Nanjing University (Natural Sciences)*, (4): 633~637.
- Sun Yan, Shu Liangshu, Faure M, Charvet J. 1997&. Tectonic development of the metamorphic core complex of the Wugongshan in the northern Jiangxi Province. *Journal of Nanjing University (Natural Sciences)*, 33(3): 447~449.
- Sylvester P J. 1998. Post-collisional strongly peraluminous granites. *Lithos*, 45(1): 29~44.
- Vervoort J D, Pachelt P J, Gehrels G E, Nutman A P. 1996. Constraints on early Earth differentiation from hafnium and neodymium isotopes. *Nature*, 379: 624~627.
- Wang Dan, Zheng Jianping, Ma Qiang, Griffin W L, Zhao Huan., Wong Jean. 2013. Early Paleozoic crustal anatexis in the intraplate Wuyi—Yunkai orogen, South China. *Lithos*, 175~176: 124~145.
- Wang Yuejun, Fan Weiming, Zhao Guochun, Ji Shaocheng, Peng Touping. 2007. Zircon U-Pb geochronology of gneissic rocks in the Yunkai massif and its implications on the Caledonian event in the South China block. *Gondwanan Research*, 12(4): 404~416.
- Wang Yuejun, Zhang Aimei, Fan Weiming, Zhao Guochun, Zhang Guowei, Zhang Yuzhi, Zhang Feifei, Li Sanzhong. 2011. Kwangssian crustal anatexis within the eastern South China Block: Geochemical, zircon U-Pb geochronological and Hf isotope fingerprints from the gneissoid granites of Wugong and Wuyi—Yunkai Domains. *Lithos*, 127: 239~260.
- Wang Yuejun, Zhang Feifei, Fan Weiming, Zhang Guowei, Chen Shiyou, Cawood P A, Zhang Aimei. 2010. Tectonic setting of the South China Block in the Early Paleozoic: Resolving intracontinental and ocean closure models from detrital zircon U-Pb geochronology. *Tectonics*, 29: 6020~6035.
- Wedepohl K H. 1995. The composition of the continental crust. *Geochimica et Cosmochimica Acta*, 59(7): 1217~1232.
- Whalen J B, Currie K L, Chappell B W. 1987. A-type granites: Geochemical characteristics, discrimination and petrogenesis. *Contrib. Mineral. Petrol.*, 95: 407~419.
- Wu Fuyuan, Li Xianhua, Yang Jinhui, Zheng Yongfei. 2007b&. Discussions on the petrogenesis of granites. *Acta Petrologica Sinica*, 23(6): 1217~1238.
- Wu Fuyuan, Li Xianhua, Zheng Yongfei, Gao Shan. 2007a&. Lu—Hf isotopic systematics and their applications in petrology. *Acta Petrologica Sinica*, 23(2): 185~220.
- Yu Yang, Huang Xiaolong, He Pengli, Li Jie. 2016. I-type granitoids associated with the Early Paleozoic intracontinental orogenic collapse along pre-existing block boundary in South China. *Lithos*, 248~252: 353~365.
- Zhang Fangrong. 2000&. The character and emplacement mechanism of gneiss in Wugong Mountain. *Journal of East China Geological Institute*, 23(2): 146~149.
- Zhang Feifei, Wang Yuejun, Fan Weiming, Zhang Aimei, Zhang Yuzhi. 2010&. LA-ICPMS zircon U-Pb geochronology of late Early Paleozoic granites in eastern Hunan and western Jiangxi provinces, South China. *Geochimica*, 39(5): 414~426.
- Zhang Feifei, Wang Yuejun, Zhang Aimei, Fan Weiming, Zhang Yuzhi, Zi Jianwei. 2012. Geochronological and geochemical constraints on the petrogenesis of Middle Paleozoic (Kwangssian) massive granites in the eastern South China Block. *Lithos*, 150: 188~208.
- Zhong Yufang, Ma Changqian, Liu Lei, Zhao Junhong, Zheng Jianping, Nong Junnian, Zhang Zejun. 2014. Ordovician appinines in the Wugongshan Domain of the Cathaysia Block, South China: Geochronological and geochemical evidence for intrusion into a local extensional zone within an intracontinental regime. *Lithos*, 198~199: 202~216.
- Zhong Yufang, Ma Changqian, Zhang Chao, Wang Shiming, She Zhenbing, Liu Lei, Xu Haijin. 2013. Zircon U-Pb age, Hf isotopic compositions and geochemistry of the Silurian Fenglingshan I-type granite pluton and Taoyuan mafic—felsic Complex at the southeastern margin of the Yangtze Block. *Journal of Asian Earth Sciences*, 74: 11~24.
- Zhong Yufang, Wang Lianxun, Zhao Junhong, Liu Lei, Ma Changqian, Zheng Jianping, Zhang Zejun, Luo Biji. 2016. Partial melting of an ancient sub-continental lithospheric mantle in the Early Paleozoic intracontinental regime and its contribution to petrogenesis of the coeval peraluminous granites in South China. *Lithos*, 264: 224~238.
- Zhou Xiaoping, Lü Junyang, Hu Bingqian, Kang Kai, Jiang Fan, Hu Liang, Zhang Na. 2022. Zircon U—Pb and Lu—Hf isotopes of Muniushan monzogranite in Xilaokou area, Jiaobei Terrane—Indicating Paleoproterozoic magmatism and crustal evolution of the North China Craton. *Geological Review*, 68(3): 891~906.

Petrological, zircon U-Pb, Lu—Hf isotopic geochemical characteristics of the Early Paleozoic granites in Wugong Mountain area, Jiangxi Province, and their geological significance

ZHANG Yaoyao^{1, 2)}, LIU Kai¹⁾, HE Qingcheng¹⁾, TONG Jue³⁾, DENG Yuefei⁴⁾, YU Chenghua⁵⁾, SUN Junliang²⁾, YU Tingxi^{1, 2)}, GUO Junhan¹⁾, WANG Shuxun²⁾

1) Chinese Academy of Geological Sciences, Beijing, 100037;

2) China University of Geosciences (Beijing), Beijing, 100083;

3) The Fourth Geological Brigade of Jiangxi Geological Bureau, Pingxiang, Jiangxi, 337000;

4) CIGIS(CHINA) LIMITED, Beijing, 100007;

5) Shenzhen Investigation and Research Institute CO., LTD, Shenzhen, Guangdong, 518000

Objectives: This paper provided Petrography, geochemical characteristics, LA-ICP-MA zircon U-Pb age, and

zircon Lu—Hf isotopes of Early Paleozoic granite in the Wugong Mountain area, South China. The formation age, genesis, and geological significance of granites are discussed.

Methods: Based on the field work, through the microscopic observation, the whole rock chemical analysis, the LA-ICP-MS zircon U-Pb isotopic chronology, and the LA-ICP-MS zircon Lu—Hf isotopes of granites.

Results: The zircons of Wugong Mountain granite have good euhedral degree and developed oscillatory belts, showing the characteristics of magmatic origin. Zircon LA-ICP-MS U-Pb isotopic chronology shows that the granites in the Wugong Mountain area were formed at 441.6~442.2 Ma and were the products of the Early Silurian orogeny. The rocks are rich in silicon ($\text{SiO}_2 = 67.43\% \sim 73.06\%$), alkali ($\text{Na}_2\text{O} + \text{K}_2\text{O} = 6.47\% \sim 8.46\%$), and poor in calcium ($\text{CaO} = 0.78\% \sim 2.64\%$), magnesium ($\text{MgO} = 0.46\% \sim 1.61\%$). Aluminum saturation index ($A/\text{CNK} = 1.09 \sim 1.35$). It is enriched in large ion lithophile elements such as Rb, K, Th and U, and relatively depleted in high field strength elements such as Nb and Ti. The ratio of light and heavy rare earth elements (La/Yb) $N = 7.91 \sim 12.69$, with a high degree of differentiation and moderate—weak negative Eu anomaly ($\delta\text{Eu} = 0.50 \sim 0.86$). The rare earth distribution curves are right-leaning, indicating the characteristics of S-type granite. Zircon $f_{\text{Lu/Hf}}$ values of the Wugong Mountain granite are all less than -0.9 , and $\varepsilon_{\text{Hf}}(t)$ are all negative.

Conclusions: Collectively, it is suggested that the granite belongs to strong peraluminous high-potassium calc-alkaline granite. It is S-type granite, and the magmatic facies is hornblende + plagioclase + garnet. The Wugong Mountain granite was formed in the Early Silurian, and the test results are relatively concentrated, revealing that the early Paleozoic granite in the Wugong Mountain area was formed in a relatively short time. The zircon Lu—Hf isotopic characteristics indicate that the magma source area is neoproterozoic continental crust material. The Wugong Mountain granite was formed in an intracontinental orogenic environment in response to the Wuyi—Yunkai orogenic stage in this area.

Keywords: Wugong Mountain; Early Paleozoic; geochemistry; Lu—Hf isotopes; geological significance

Acknowledgements: We sincerely thank anonymous reviewers and editors for their critical comments and constructive suggestions, which have greatly improved the quality of this paper. This research is financially supported by the project of China Geological Survey (No. DD20221677-2 and DD20201165), fundamental research funds of Central Finance (JKY202004, JKY202011), Key Research and Development Project of Jiangxi Province (No. 20203BBG72W011) and Science and Technology Research Project of Jiangxi Geological Bureau (No. 2021AA07).

First author: ZHANG Yaoyao, male, born in 1987, senior engineer, is mainly engaged in ore field structure and regional geological survey research; Email: zhangyy@cags.ac.cn

Corresponding author: LIU Kai, male, born in 1983, professor level senior engineer, mainly engaged in regional geological survey research work. Email: acancer@163.com

Manuscript received on: 2022-06-10; **Accepted on:** 2022-12-21; **Published online on:** 2023-01-20

Doi: 10.16509/j.georeview.2023.01.025

Edited by: ZHANG Yuxu